Chemosphere 261 (2020) 127729

Contents lists available at ScienceDirect

Chemosphere

journal homepage: www.elsevier.com/locate/chemosphere

Effect of emission control measures on ozone concentrations in Hangzhou during G20 meeting in 2016

Ye Wang, Hong Liao*

Jiangsu Key Laboratory of Atmospheric Environment Monitoring and Pollution Control, Jiangsu Collaborative Innovation Center of Atmospheric Environment and Equipment Technology, School of Environmental Science and Engineering, Nanjing University of Information Science & Technology, Nanjing 210044, China

HIGHLIGHTS

- MDA8 O_3 concentrations in Hangzhou during G20 exceeded national air quality standard.
- Emission control measures during G20 reduced MDA8 O_3 level in Hangzhou by 11.7%.
- Emission controls in industry and transportation sectors are most effective for controlling O_3.

ARTICLE INFO

Article history:
Received 20 March 2020
Received in revised form
13 July 2020
Accepted 14 July 2020
Available online 29 July 2020

Handling Editor: Chennai Guest Editor

Keywords:
O_3 pollution
G20 meeting
Emission control
Sectoral contribution

ABSTRACT

The effect of emission control measures on ozone (O_3) concentrations in Hangzhou during G20 (The Group of Twenty Finance Ministers and Central Bank Governors) meeting during 24 August to 6 September of 2016 was evaluated using the nested version of a global chemical transport model. During G20, observed concentrations of PM_{10}, $PM_{2.5}$, SO_2, NO_2, and CO were all below national air quality standards, whereas those of MDA8 O_3 were above national standard (with an averaged value of 160.2 μg m^{-3}) but had a decreasing trend. Model sensitivity studies show that, MDA8 O_3 concentrations in Hangzhou during G20 were reduced by 11.3 μg m^{-3} (6.8%), 14.8 μg m^{-3} (8.9%), and 19.5 μg m^{-3} (11.7%) with emission control measures in the core area, Zhejiang province, and the Yangtze River Delta (YRD) region, respectively, indicating that control measures were the most effective when carried out jointly in YRD. Considering the ratios of NO_x to VOCs during G20, Hangzhou and most areas of Zhejiang province were in transitional regime; reductions in either NO_x or VOCs could reduce O_3 concentrations. We also quantified how sensitive O_3 concentrations respond to emission reductions in sectors of industry, power, residential and transportation in the whole of YRD during G20. The removal of emissions in industry and transportation sectors would lead to the largest reductions of 17.6 μg m^{-3} (10.5%) and 12.3 μg m^{-3} (7.4%) in MDA8 O_3 concentrations in Hangzhou during G20, respectively. This study has important implications for the control of high O_3 levels in eastern China.

1. Introduction

Air quality in China has drawn a lot of attention because of the high concentrations of $PM_{2.5}$ and ozone (O_3) resulted from its rapid economic development. The Chinese government launched the 'Air Pollution Prevention and Control Action Plan' to reduce anthropogenic emissions to improve air quality in 2013. According to the 'Environmental and Ecological Status Bulletins in China' (http://www.mee.gov.cn/hjzl/), from 2013 to 2017, mean concentrations of $PM_{2.5}$, PM_{10}, SO_2, NO_2 and CO in 74 major cities decreased by 34.7%, 32.2%, 57.5%, 9.1% and 32.0%, respectively, but the 90th percentile concentration of the maximum daily 8-h average of O_3 concentration (MDA8 O_3) averaged over these cities increased by 20.1%. Under the background of increasingly serious O_3 pollution in China, G20 meeting offers a good opportunity to study whether O_3 concentrations can be controlled effectively in summer in the polluted eastern China.

In recent years, several significant events were held in China successfully, such as the Beijing Olympic Games in 2008, the Shanghai World Expo in 2010, the Asia-Pacific Economic

* Corresponding author. No.219, Ningliu Road, Nangjing, 210044, China.
E-mail address: hongliao@nuist.edu.cn (H. Liao).

https://doi.org/10.1016/j.chemosphere.2020.127729
0045-6535/

Cooperation (APEC) conference in 2014, the Victory Day Parade (V-Day Parade) in 2015, and the Group of Twenty Finance Ministers and Central Bank Governors (G20) summit in 2016. For purpose of ensuring good air quality during these important events, air quality control measures were implemented before and during the events, which were proved to be very effective by measured concentrations of air pollutants. A number of studies were carried out to quantify the effectiveness of the control measures during these events. For example, Gao et al. (2011) reported by using the Weather Research and Forecasting model coupled to Chemistry (WRF-Chem) that $PM_{2.5}$ concentrations in Beijing decreased by about 30%, as a result of the reductions in anthropogenic emissions by about 50%, 35%, and 10% in Beijing, Hebei province, and other nearby regions, respectively, during the Beijing Olympic Games in 8–24 August 2008. Wang et al. (2010) used the fifth-generation NCAR/Penn State Mesoscale Model and Community Multi-scale Air Quality (MM5-CMAQ) model to simulate the reductions of pollutants during the Beijing Olympic Games and showed that, with emissions of SO_2, NO_x, PM_{10}, and NMVOCs reduced by 41%, 47%, 55%, and 57%, respectively, $PM_{2.5}$ concentrations during the Olympic Games were reduced by about 60% compared to concentrations in June of 2008. Huang et al. (2017) quantified the effects of local emission reductions during the 2014 Nanjing Youth Olympic Games (NYOG) by using the Weather Research and Forecast and Community Multi-scale Air Quality (WRF-CMAQ) model. Under an unfavorable weather condition during NYOG (1–31 August, 2014), simulated mean concentrations of SO_2, NO_2, PM_{10}, $PM_{2.5}$, and CO decreased by 24.6%, 12.1%, 15.1%, 8.1%, and 7.2% when emissions of these species were reduced by 25.0%, 15.0%, 42.8%, 32.6%, and 20.0%, respectively. Liang et al. (2017) estimated the effectiveness of emission reductions during 2014 APEC meeting (3–12 November, 2014) and 2015 Victory Day Parade (20 August to 3 September, 2015) by using a generalized linear regression model (GLM). They found that the meteorological conditions and pollution control strategies contributed, respectively, 30% and 28% to the reductions of $PM_{2.5}$ concentrations during APEC and 38% and 25% to those during the Victory Parade.

Although the above-mentioned emission reductions were very effective in reducing $PM_{2.5}$ concentrations during those events, previous studies revealed that O_3 concentrations increased or remained unchanged during some events. For instance, Tang et al. (2017) examined the sensitivity of O_3 to emission reductions during the Beijing Olympic Games by using the MM5-CMAQ model. They found that the average O_3 concentration increased by 8 ppbv in urban Beijing where NO_x decreased by about 15 ppbv during the Olympics, indicating the impact of titration effect. Xu et al. (2016) also reported on the basis of observations that emission reductions during Beijing Olympics had a small impact on O_3 concentrations; averaged concentration of O_3 in Beijing and its surroundings was reduced by about 1% with a 33% decrease in NO_x concentration, suggesting that O_3 production was VOC-limited. Guo et al. (2016) used the WRF-Chem model to evaluate the effect of district-joint emission controls on air quality during 2014 APEC meeting. Emission reductions from sectors of industry, residential, and transportation in urban Beijing and Huairou were 50%, 40% and 40%, respectively, which led to decreases in concentrations of $PM_{2.5}$, PM_{10}, NO_2, and CO by 22%, 24%, 10% and 22%, respectively, whereas mean O_3 concentration increased by 24% due to the reductions in NO_2. Li et al. (2017c) reported similar results; the emission control during APEC increased O_3 concentration by 58.2% because the degree of NO_x reduction exceeded that of VOCs.

The Group of twenty (G20) was formally established in 1999, which comprises 19 countries plus the European Union. The G20 summit provided the opportunity for G20 members to explore approaches to the economic cooperation for the world economy. G20 took place in Hangzhou (119.8°E, 30.4°N), the capital city of Zhejiang province in the Yangtze River Delta region (YRD), during 4–5 September, 2016. In order to ensure the 'blue sky' during the conference, the government of Zhejiang province carried out a series of district-joint air quality control measures which took Hangzhou as the core city and radiated to other cities in Zhejiang and neighbor provinces. The areas that implemented the air pollution control measures included the core area (CRA), the strictly controlled area (SCA), the controlled area in Zhejiang (CAZJ) and the controlled area in Yangtze River Delta except Zhejiang (CAYRD-ZJ) (Fig. 1). Most stringent control measures were carried out in CRA, followed by the other three areas. The measures aimed to reduce emissions from industry, transportation, residential and power sectors (Yu et al., 2018). With the emission control measures, concentrations of all routine pollutants except for O_3 ($PM_{2.5}$, PM_{10}, SO_2, NO_2, and CO) during G20 met the National air quality standards.

There were several studies about the effectiveness of emission control measures during G20. Su et al. (2017) used lidar data to analyze the difference in concentrations of aerosols and O_3 between G20 and post-G20 period, and found that aerosol extinction coefficient during G20 was 50% lower than that in post-G20 period in the lower lidar layer, while O_3 concentration during G20 was 37% higher than that in post-G20 period. Mao and Hu (2017) reported that, compared with September 2015 and August 2016, the monthly average Air Quality Index (AQI) during G20 were lower by 35 and 25 in the core area and lower by 20 and 25 in the strictly controlled area. Li et al. (2017b) used WRF-CMAQ model to evaluate the effect of emission controls on $PM_{2.5}$ and O_3 and concluded that

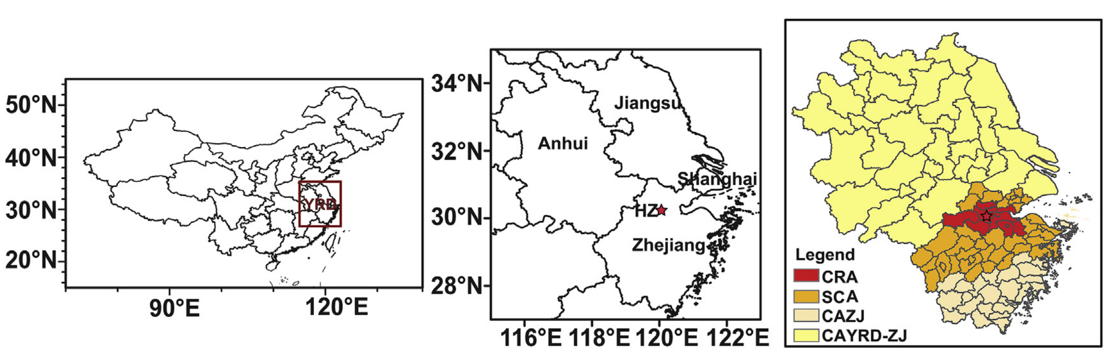

Fig. 1. The areas implemented control measures during G20 meeting. YRD consists of Zhejiang province, Jiangsu province, Anhui province and Shanghai (left and middle panels). The core area (CRA), the strictly controlled area (SCA), the controlled area in Zhejiang (CAZJ) and the controlled area in Yangtze River Delta except Zhejiang (CAYRD-ZJ) are shown in the right panel. The red star in the right two panels indicates the location of Hangzhou. (For interpretation of the references to color in this figure legend, the reader is referred to the Web version of this article.)

simulated concentrations of $PM_{2.5}$ and O_3 decreased by 56% and 25%, respectively, as a result of reductions in emissions from power plants and industry by 40% in Shanghai, Jiangsu and Anhui provinces and by 50% in Zhejiang province during August 24 to September 6. However, previous studies about G20 did not examine the effectiveness of local and joint emission control measures for O_3 as well as the sensitivity of O_3 concentrations to emission reductions in different sectors. We present results of such a study here by using a global 3-D model of atmospheric chemistry driven by meteorological input from the Goddard Earth Observing System (GEOS-Chem).

The descriptions of the GEOS-Chem model, emissions, observations, and numerical experiments are presented in Section 2. Section 3 presents the analyses of observed meteorological conditions and concentrations of pollutants, model evaluation, as well as the simulated changes in O_3 with reductions in emissions. Section 4 summarizes the main conclusions.

2. Method

2.1. The GEOS-Chem model

The simulation of air quality during G20 is carried out by using the GEOS-Chem model version11-01 (http://wiki.seas.harvard.edu/geos-chem/index.php/GEOS-Chem_v11-01), which is a global 3-D chemical transport model (CTM) driven by meteorological fields from the Modern-Era Retrospective Analysis for Research and Applications, version 2 (MERRA-2) provided by the Global Modelling and Assimilation Office (GMAO). The model includes fully coupled O_3-NO_x-hydrocarbon chemistry (Bey et al., 2001; Park et al., 2004) and aerosols including sulfate (Park et al., 2004), nitrate (Pye et al., 2009), ammonium, black carbon and organic carbon (Park et al., 2003), mineral dust (Fairlie et al., 2007), and sea salt (Alexander et al., 2005). Photolysis rates are calculated by Fast-JX scheme (Bian and Prather, 2002). Heterogeneous reactions of aerosols, such as the irreversible absorption of NO_3 and NO_2 on wet aerosols (Jacob, 2000), hydrolysis of N_2O_5 (Evans and Jacob, 2005), and the uptake of HO_2 by aerosols (Thornton et al., 2008) are included. Wet deposition in the GEOS-Chem model, including scavenging in convective updrafts, rainout, and wash out, follows the scheme described by Liu et al. (2001) and applies only to soluble aerosols and gases. Dry deposition is computed based on the resistance-in-series scheme of Wesely (1989). The nested domain for Asia (70°-150°E, 10°S-55°N) has a horizontal resolution of 0.5° latitude by 0.625° longitude and 47 vertical layers up to 0.01 hPa. Tracer concentrations at the lateral boundaries are provided by a global GEOS-Chem simulation at 2° latitude by 2.5° longitude horizontal resolution. The GEOS-Chem model has been used extensively for studying air quality in China, including haze pollution (Huang et al., 2014; Zhang et al., 2015, 2016; Yang et al., 2016; Li et al., 2016a; Qiu et al., 2017; Cai et al., 2017), O_3 air quality (Fu et al., 2009; Yang et al., 2014; Zhu and Liao, 2016; Ni et al., 2018a), and the effectiveness of emission controls during the Olympics (Wang et al., 2009) and APEC meeting (Gu and Liao, 2016).

2.2. Emissions

Muti-resolution Emission Inventory for China (MEIC) for year 2016 is used in our simulations. The inventory has a resolution of 0.25° × 0.25° and is downloaded from www.meicmodel.org/dataset-meic.html. Fig. 2 shows the spatial distributions of NO_x and anthropogenic non-methane volatile organic carbons (NMVOCs) for August of 2016. In YRD, regions with high emissions are Shanghai, southern Jiangsu, central Anhui and northeastern Zhejiang.

Table 1 shows anthropogenic emissions of O_3 precursors, aerosols and aerosol precursors in regions of CRA, SCA, CAZJ and CAYRD-ZJ during 24 August to 6 September of 2016 from the MEIC inventory. Emissions of CO, NO_x, and NMVOCs were the highest among all species, which were 622.5×10^3 kg, 136.4×10^3 kg, and 78.9×10^3 kgC in YRD (YRD = CRA + SCA + CAZJ + CAYRD-ZJ), respectively. Emissions of NO_x were mainly from industry (52.3×10^3 kg) and transportation (50.8×10^3 kg) sectors, accounting for 38.4% and 37.2% of total NO_x emissions in YRD during G20, respectively. Sectors of industry, transportation, residential, and power contributed 68.3%, 0.2%, 10.5% and 21.0%, respectively, to total NMVOCs emissions in YRD during G20.

The percentages of emission reductions for different species and in different sectors for periods of 24–27 August and 28 August-6 September are taken from Environmental Quality Guarantee Scheme during G20 in 2016 (Yu et al., 2018) (Table 1). The industry sector had the largest percentage reductions in emissions during

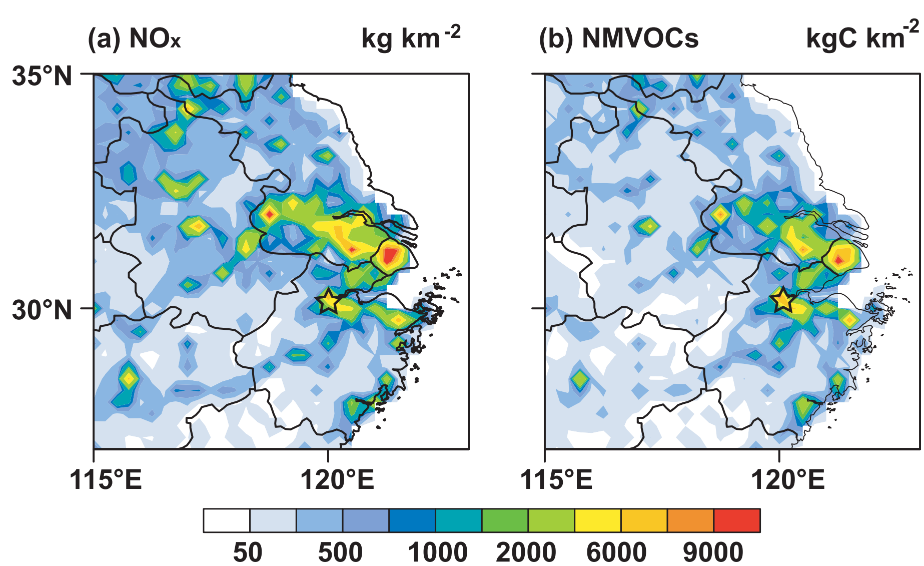

Fig. 2. Anthropogenic emissions of (a) NO_x and (b) NMVOCs in YRD in August, 2016. The black star indicates the location of Hangzhou.

Table 1
Total anthropogenic emissions of O_3 precursors, aerosols and aerosol precursors in the regions of CRA, Zhejiang province, and YRD for emission-controlled period of 24 August to 6 September (units: 10^3 kgC for NMVOCs and 10^3 kg for other species). Emissions are taken from MEIC for 2016, and emission reductions in percentages are taken from Environmental Quality Guarantee Scheme during G20 in 2016 (Yu et al., 2018).

Period		24–27 August				28 August - 6 September				
Sector		Industry	Power	Residential	Transport	Industry	Power	Residential	Transport	Total
Emissions in CRA	NO_x	1.37	0.54	0.02	0.98	3.53	1.15	0.04	2.50	10.13
	NMVOCs	2.43	0.003	0.17	0.66	5.03	0.01	0.35	1.28	9.93
	CO	5.33	0.42	0.58	5.64	13.65	0.90	1.45	14.36	42.34
	SO_2	0.76	0.16	0.02	0.05	1.94	0.35	0.06	0.13	3.47
	BC	0.04	0	0.01	0.03	0.1	0	0.02	0.08	0.28
	OC	0.03	0	0.02	0.01	0.08	0	0.04	0.03	0.21
	Reductions	100%	50%	50%	0%	100%	50%	50%	50%	–
Emissions in SCA	NO_x	1.64	1.35	0.03	1.46	4.24	2.89	0.07	3.72	15.40
	NMVOCs	2.83	0.01	0.24	0.91	5.86	0.01	0.49	1.78	12.13
	CO	6.80	1.63	1.36	7.86	17.42	3.48	3.41	20.00	61.95
	SO_2	0.91	0.4	0.04	0.08	2.33	0.85	0.09	0.19	4.89
	BC	0.05	0	0.02	0.05	0.12	0	0.04	0.12	0.40
	OC	0.04	0	0.05	0.02	0.1	0	0.12	0.05	0.38
	Reductions	50%	30%	30%	0%	50%	30%	30%	50%	–
Emissions in CAZJ	NO_x	0.87	0.5	0.02	0.9	2.26	1.09	0.06	2.3	8.00
	NMVOCs	1.56	0.003	0.19	0.58	3.23	0.01	0.38	1.12	7.07
	CO	3.34	1.08	1.05	4.96	8.54	2.36	2.62	12.62	36.58
	SO_2	0.48	0.13	0.03	0.05	1.23	0.28	0.07	0.12	2.39
	BC	0.02	0	0.01	0.03	0.06	0	0.03	0.07	0.22
	OC	0.02	0	0.04	0.01	0.05	0	0.09	0.03	0.24
	Reductions	50%	30%	30%	0%	50%	30%	30%	0%	–
Emissions in CAYRD-ZJ	NO_x	10.58	7.5	0.41	10.96	27.81	16.61	1.03	27.94	102.84
	NMVOCs	10.63	0.04	2.14	3.38	22.29	0.08	4.3	6.86	49.72
	CO	65.17	8.94	31.04	30.98	169.12	19.82	77.59	78.98	481.63
	SO_2	5.46	2.13	0.3	0.44	14.18	4.7	0.74	1.12	29.07
	BC	0.38	0	0.3	0.4	1.01	0	0.76	1.02	3.87
	OC	0.34	0	1.11	0.14	0.9	0	2.79	0.37	5.65
	Reductions	40%	30%	0%	0%	40%	30%	0%	0%	–

G20. Emissions of NO_x (NMVOCs) in CRA, Zhejiang province, and YRD were reduced by 69.3% (84.3%), 45.3% (56.3%), and 27.7% (37.5%), respectively, during G20.

2.3. Observations

The observed hourly concentrations of air pollutants are obtained from China's Ministry of Ecology and Environment and can be downloaded from beijingair.sinaapp.com. There are 11 observational sites in Hangzhou (Table 2), 10 of which are urban sites and one is a rural site. Daily mean values of $PM_{2.5}$, PM_{10}, SO_2, CO, NO_2, and MDA8 O_3 concentrations are calculated and used for model evaluation. The observed hourly meteorological parameters (temperature, relative humidity, wind, precipitation) are from Mantoushan monitoring station which is a national reference climate station.

Table 2
Locations of observational sites in Hangzhou.

Sites	Longitude (°E)	Latitude (°N)
Binjiang[a]	120.22	30.21
Xixi[a]	120.06	30.27
Qiandao Lake[b]	119.03	29.64
Xiasha[a]	120.38	30.31
Wolong Bridge[a]	120.13	30.25
Zhejiang Agricultural University[a]	120.19	30.27
Zhaohui Wuqu[a]	120.16	30.29
Hemu Primary School[a]	120.12	30.31
Linping Town[a]	120.30	30.42
Chengxiang Town[a]	120.27	30.18
Yunxi[a]	120.09	30.18

[a] Urban sites.
[b] Rural sites.

2.4. Numerical experiments

The simulations of air pollutants are carried out for the time period of 10 August to 20 September, which are further classified as the periods of before G20 (PREG20, 10–23 August), during G20 (24 August to 6 September), and after G20 (POSTG20, 7–20 September). To compare the effects of local and joint emission controls, four numerical experiments are conducted (Table 3):

(1) BASE: Baseline simulation without emission control measures from 10 August to 20 September;
(2) CTRL_CRA: Same as BASE simulation but with emission control in CRA during G20;
(3) CTRL_ZJ: Same as BASE simulation but with emission control over Zhejiang province during G20;
(4) CTRL_YRD: Same as BASE simulation but with emission control in YRD during G20;

Four more numerical experiments are conducted to quantify the sensitivity of O_3 concentrations to emission reductions in different sectors from 24 August to 6 September (Table 3):

(5) CTRL_noIND: Same as BASE simulation but no emissions from industry sector in YRD;
(6) CTRL_noPOW: Same as BASE simulation but no emissions from power sector in YRD;
(7) CTRL_noRES: Same as BASE simulation but no emissions from residential sector in YRD;
(8) CTRL_noTRA: Same as BASE simulation but no emissions from transportation sector in YRD.

All the simulations are driven by the assimilated MERRA-2 meteorological fields and there is a three-month spin-up before August 24 of 2016.

Table 3
Summary of numerical experiments.

Simulation	Simulated time period	Sectors with emission control	Area with emission control
BASE	10 August-20 September	Without control	Without control
CTRL_CRA	24 August-6 September	Industry, Power, Residential, Transport	CRA[a]
CTRL_ZJ	24 August-6 September	Industry, Power, Residential, Transport	Zhejiang province[b]
CTRL_YRD[d]	24 August-6 September	Industry, Power, Residential, Transport	YRD[c]
CTRL_noIND	24 August-6 September	Industry	YRD
CTRL_noPOW	24 August-6 September	Power	YRD
CTRL_noRES	24 August-6 September	Residential	YRD
CTRL_noTRA	24 August-6 September	Transport	YRD

[a] Red area in the right panel of Fig. 1.
[b] Red plus orange plus light yellow areas in the right panel of Fig. 1.
[c] All colored areas under emission control in the right panel of Fig. 1.
[d] Control measures in CTRL_YRD simulation were actually conducted during G20 meeting.

3. Results

3.1. Observed meteorological parameters and concentrations of pollutants

Fig. 3 shows the variations of temperature, precipitation, relative humidity, wind speed and wind direction in Hangzhou from 10 August to 20 September in 2016. During G20 (24 August to 6 September), mean temperature was 27.4 °C, which was 12.7% lower than that in PREG20 (31.4 °C) and 15.6% higher than the value in POSTG20 (23.7 °C). Averaged relative humidity during G20 was 60.4%, which was the lowest value among the three periods (it was 71.7% in PREG20 and 79.2% in POSTG20). The accumulated precipitation reached 49.5, 16.9, and 153.6 mm in PREG20, G20, and POSTG20, respectively. Daily wind speeds in the whole period (10 August-20 September) were generally low and most of them were lower than 4 m s^{-1}. The mean wind speed during G20 was 2.6 m s^{-1}, which was higher than that in PREG20 (2.1 m s^{-1}). The period of G20 had high temperature, low relative humidity, and low wind speed, which were favorable for O_3 formation as reported by Gong and Liao (2019) on the basis of the analysis of all observed O_3 pollution events in eastern China during 2014–2017.

Fig. 4 shows the observed daily surface concentrations of pollutants ($PM_{2.5}$, PM_{10}, SO_2, NO_2, CO, MDA8 O_3) in Hangzhou from 10 August to 20 September of 2016. During G20, concentrations of all pollutants, except for O_3, were kept below national air quality standards. Relative to PREG20, regional mean concentrations of $PM_{2.5}$, PM_{10}, SO_2, NO_2, CO, and MDA8 O_3 in Hangzhou (YRD) changed by +3.3 (+8.9) μg m^{-3}, +4.0 (+16.7) μg m^{-3}, +0.6 (+3.4) μg m^{-3}, -4.6 (+6.8) μg m^{-3}, +0.06 (+0.08) mg m^{-3}, and +11.6 (+36.6) μg m^{-3}, respectively (Fig. S1). Therefore, concentrations of all species increased over the YRD and the magnitudes of increases were larger than those of increases in Hangzhou. Concentration of NO_2 in Hangzhou showed decrease relative to PREG20. These changes indicate the effectiveness of control measures in Hangzhou. The overall increases in concentrations in YRD during G20

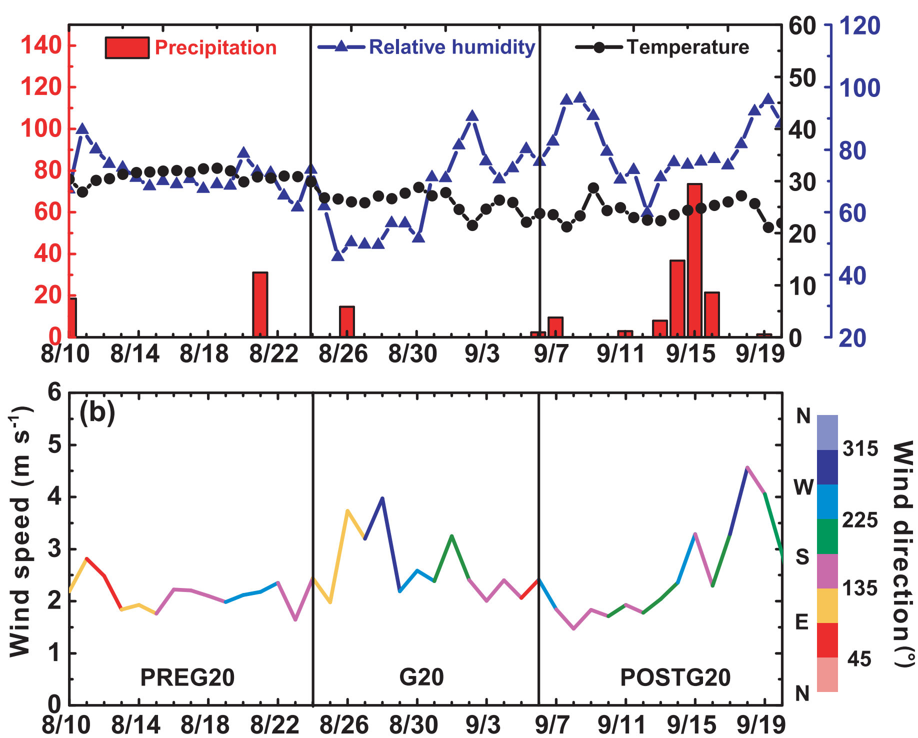

Fig. 3. (a) Time series of observed daily precipitation (red bars), relative humidity (blue line with triangles), temperature (black line with dots) at Mantoushan station in Hangzhou from 10 August to 20 September of 2016. (b) Time series of observed daily wind. The values are wind speeds and the colors show wind directions. (For interpretation of the references to color in this figure legend, the reader is referred to the Web version of this article.)

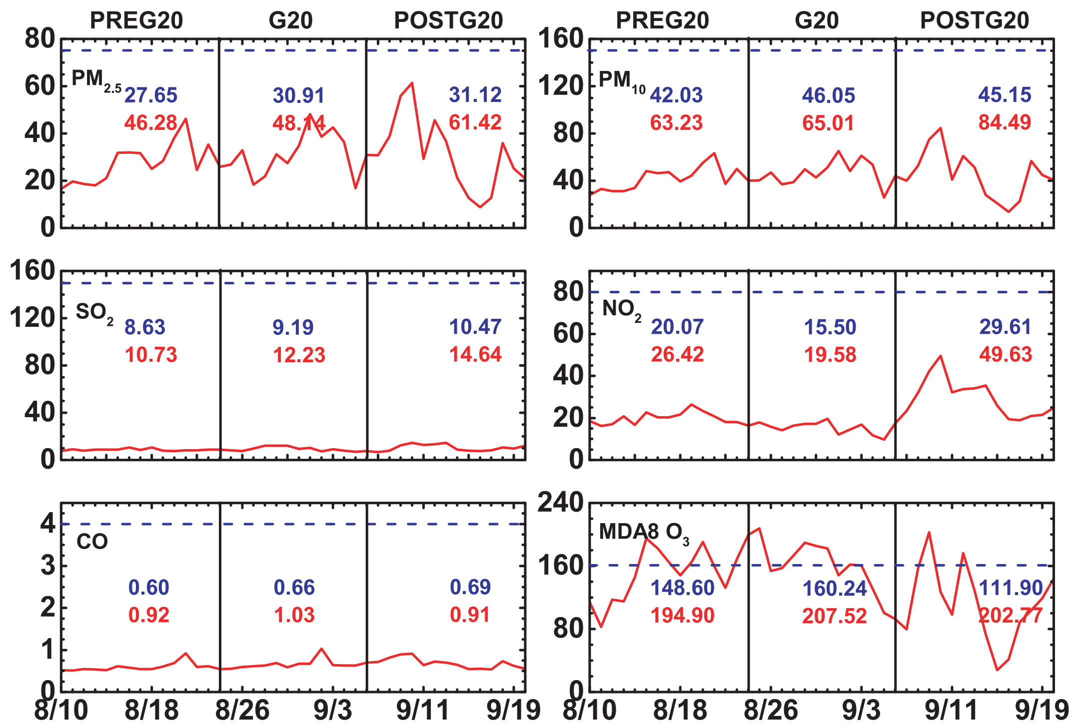

Fig. 4. Observed daily surface concentrations (red lines) of $PM_{2.5}$, PM_{10}, SO_2, NO_2, CO and MDA8 O_3 averaged over 11 sites in Hangzhou (Table 2) during 10 August to 20 September, 2016. The numbers indicate mean (blue) and maximum (red) concentrations of pollutants before, during and after G20 meeting. Units are mg m^{-3} for CO and μg m^{-3} for others. The blue dashed line in each panel represents national standard for the pollutant (75 μg m^{-3} for $PM_{2.5}$, 150 μg m^{-3} for PM_{10}, 150 μg m^{-3} for SO_2, 80 μg m^{-3} for NO_2, 4 mg m^{-3} for CO, and 160 μg m^{-3} for MDA8 O_3). (For interpretation of the references to color in this figure legend, the reader is referred to the Web version of this article.)

relative to PREG20 were caused by meteorological conditions. As shown in Fig. S2, southeasterlies in PREG20 brought fresh air mass to YRD, while northerlies during G20 carried pollutants to YRD from polluted areas such as the North China Plain (NCP) and Henan province (Ni et al., 2018b; Zhang et al., 2020).The observed concentrations of all pollutants increased in the beginning of POSTG20. Therefore, the scientific question is whether the control measures reduced O_3 concentrations during the meeting or not.

3.2. Evaluation of model performance

3.2.1. Evaluation of MERRA-2 meteorological parameters

Fig. 5 shows the comparisons of MERRA-2 meteorological parameters with observations at the location of Hangzhou (119.8°E, 30.4°N) for sea-level pressure (SLP), relative humidity (RH), 2-m temperature (T2M), 10-m wind speed (WS) and 10-m wind direction from 10 August to 20 September of 2016. The observed parameters are averaged every 3 h to be consistent with the 3-h time resolution of MERRA-2. During 10 August to 20 September, MERRA-2 meteorological fields agree closely with measurements, with normalized mean biases (NMB $= \frac{\sum_{i=1}^{n}(M_i - O_i)}{\sum_{i=1}^{n} O_i} \times 100\%$; M_i and O_i are the MERRA-2 (simulated) value and observed value of a meteorological parameter (pollutant concentration) at time (or site) i, respectively, and n is total number of samples) of 4.0%, −0.2%, −3.3%, 5.0% and −52.0% for SLP, RH, T2M, WS, and WD, respectively. During G20, the correlations between MERRA-2 and observed meteorological parameters were in the range of 0.54–0.99, indicating that the MERRA-2 meteorological parameters in Hangzhou agreed reasonably well with observations.

3.2.2. Evaluation of simulated MDA8 O_3 from the CTRL_YRD simulation

Fig. 6a shows the comparison of simulated and observed MDA8 O_3 concentrations in Hangzhou from 10 August to 20 September. Simulated magnitude and variation in MDA8 O_3 concentrations agree closely with observations in Hangzhou. In the periods of PREG20 (simulated by BASE), G20 (simulated by CTRL_YRD), and POSTG20 (simulated by BASE), MDA8 O_3 concentrations have NMBs of 12.3%, −8.0%, and 31.1%, respectively. The correlation coefficients of MDA8 O_3 concentrations between BASE and observations are 0.70, 0.81, and 0.80 in these three time periods, respectively. Fig. 6b and c compare the spatial distributions of MDA8 O_3 concentrations in YRD simulated by CTRL_YRD with observations for 25 August (the second day of G20 period) and 6 September (the final day of G20). On 25 August, observed and simulated MDA8 O_3 concentrations were high (exceeding 150 μg m^{-3}) over a large area that covered provinces of Anhui, Jiangsu, and northern Zhejiang. The model captures fairly well the high MDA8 O_3 concentrations on 25 August (with r of 0.43 and NMB of −8.9%) and the low concentrations on 6 September (with r of 0.66 and NMB of 25.7%) considering all the observational sites in YRD.

The model performance shown here is similar to that of GEOS-Chem model reported in studies of Gu and Liao (2016) and Zhu et al. (2019). The correlation coefficients between observed and simulated pollutants (CO, NO_2, SO_2, and $PM_{2.5}$) were in the range of 0.44–0.83 during APEC (Gu and Liao, 2016). The correlation coefficients (NMBs) between observed and simulated concentrations were 0.52 (−22.2%), 0.65 (+7.1%), 0.71 (−37.6%) for $PM_{2.5}$ and 0.91 (+25.0%), 0.86 (+31.9%), 0.85 (+20.7%) for MDA8 O_3 in Shanghai, Jiangyin, and Wenzhou, respectively, in July of 2016 (Zhu et al., 2019).

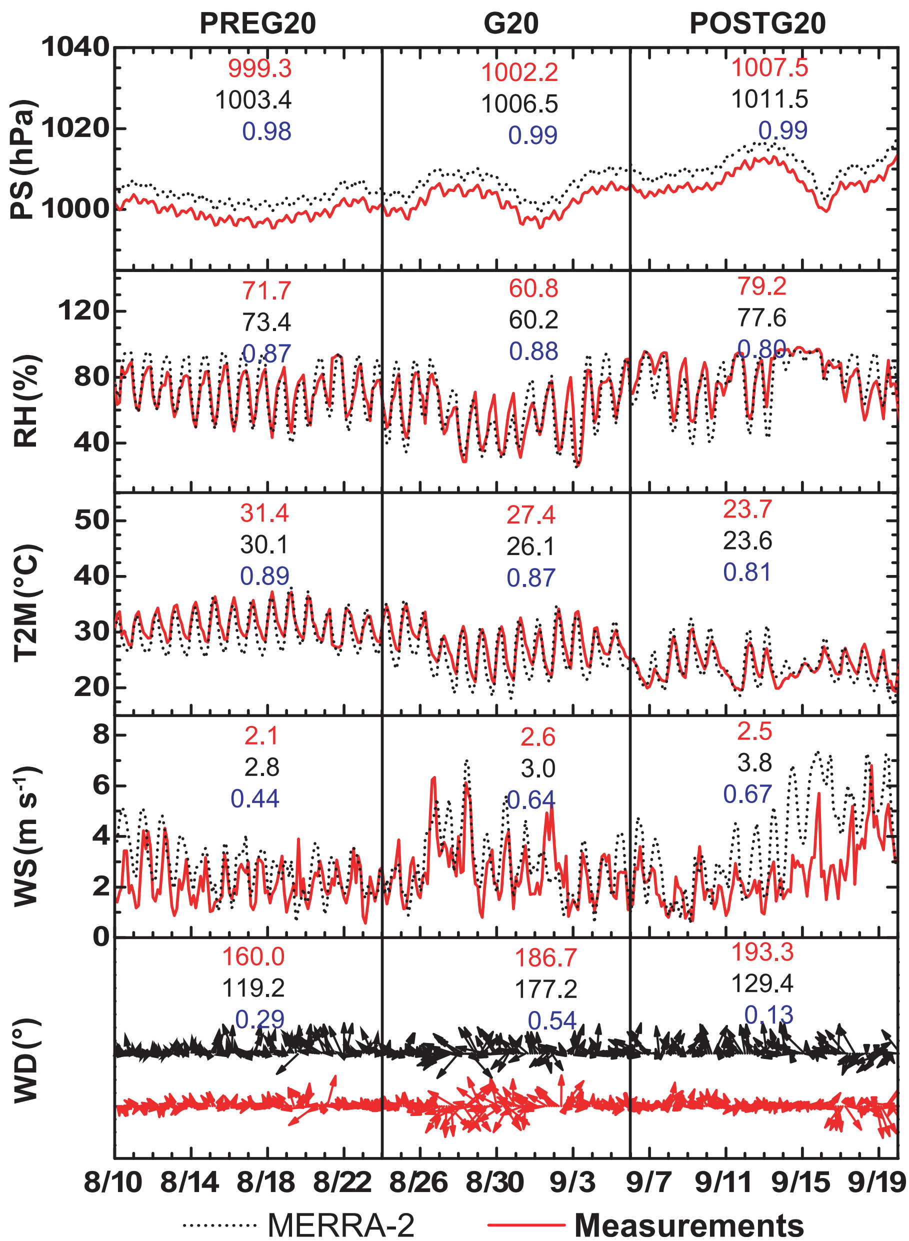

Fig. 5. Comparisons of MERRA-2 (black) and observed (red) sea-level pressure (SLP), relative humidity (RH), 2-m temperature (T2M), 10-m wind speed (WS) and 10-m wind direction (WD), at Mantoushan station in Hangzhou, from 10 August to 20 September of 2016. For each time period, the black, red, and blue numbers are the average of MERRA-2 variable, the average of observed value, and correlation coefficients (R) between measurements and MERRA-2 data, respectively. (For interpretation of the references to color in this figure legend, the reader is referred to the Web version of this article.)

3.3. Impact of district-joint control on O_3 concentrations during G20

Three numerical experiments (CTRL_CRA, CTRL_ZJ and CTRL_YRD) are conducted to quantify the impacts of control measures on O_3 during G20 as described in Section 2.4. Fig. 7a-c (Fig. 7d-f) show, relative to the BASE simulation, the absolute (percentage) changes in MDA8 O_3 concentrations resulting from emission controls in core area (CRA, red area in the right panel of Fig. 1), in the whole of Zhejiang Province (red plus orange plus light yellow areas in the right panel of Fig. 1), and in the whole of YRD (all colored areas in the right panel of Fig. 1), respectively, and concentrations are averaged over 24 August to 6 September. The largest reductions in MDA8 O_3 concentrations are simulated in northern Zhejiang province. Compared to the BASE simulation, highest reductions in MDA8 O_3 concentrations are simulated to be, 15.6 μg m^{-3} (8.0%), 21.9 μg m^{-3} (11.7%), and 26.0 μg m^{-3} (14.0%) in simulations of CTRL_CRA, CTRL_ZJ, and CTRL_YRD, respectively. It should be noted that the location of highest reduction in MDA8 O_3 is simulated to be south of the core area, as a result of the high MDA8 O_3 concentrations in that location simulated by BASE because of high emissions of biogenic VOCs (Li et al., 2016b) and the prevailing northerlies at 850 hPa during G20 (Fig. S3a). At Hangzhou, averaged over 24 August to 6 September, while MDA8 O_3 concentration was 160.2 μg m^{-3} from observations, simulated values are 166.9, 155.6, 152.1, and 147.4 μg m^{-3} in the BASE, CTRL_CRA, CTRL_ZJ, and CTRL_YRD simulations (Fig. 7d), respectively. Control measures in CRA, Zhejiang province, and YRD are

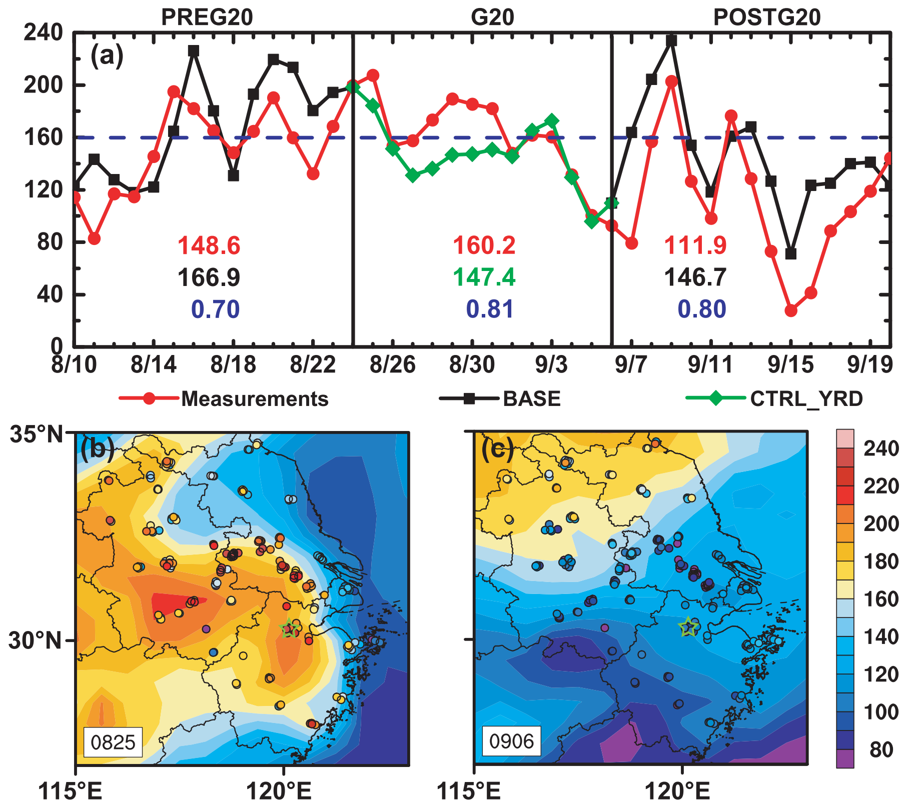

Fig. 6. (a) Comparison of daily MDA8 O_3 concentrations (μg m^{-3}) from simulations (BASE: black line with squares; CTRL_YRD: green line with diamonds) with observations (red line with dots) in Hangzhou from 10 August to 20 September of 2016. Blue dashed line represents national standard for O_3. For each period of PREG20, G20, and POSTG20, mean concentration (μg m^{-3}; red, black, and green number for observations, BASE and CTRL_YRD simulations, respectively) of MDA8 O_3 as well as the correlation coefficient between simulated and observed MDA8 O_3 concentrations (blue) are indicated. Spatial distributions of simulated (shades) by CTRL_YRD and observed (dots) concentrations of MDA8 O_3 (μg m^{-3}) in YRD are shown for (b) 25 August and (c) 6 September. The star indicates the location of Hangzhou. (For interpretation of the references to color in this figure legend, the reader is referred to the Web version of this article.)

simulated to lead to, respectively, 6.8%, 8.9%, and 11.7% of reductions in averaged MDA8 O_3 in Hangzhou during G20 relative to the BASE simulation. These results suggest that the emission control measures reduced O_3 concentrations in Hangzhou effectively although O_3 concentrations with emission controls still exceeded the national standard of 160 μg m^{-3} during G20. The reductions in O_3 concentrations with emission controls in YRD are higher than those with controls in core areas or in the whole of Zhejiang province, indicating the effectiveness of district-joint emission control measures. These model results also suggest that, in reality, regions to carry out emission control can be decided on the basis of the targeted magnitude of reduction in O_3, since emission control in the core area alone improved O_3 pollution in Hangzhou.

3.4. VOCs-NO_x-O_3 sensitivity during G20

As the most important precursors of O_3, NO_x ($NO + NO_2$) and VOCs play crucial roles in the formation of tropospheric O_3, and controlling them properly can reduce O_3 concentration effectively (Rabl and Eyre, 1998; Atkinson, 2000; Shao et al., 2009; Wei et al., 2014). O_3 formation is a highly nonlinear process. The O_3-precursors relationship can be classified into the NO_x-limited, VOC-limited, and transitional regimes quantified by VOCs/NO_x ratios (Sillman, 1999; Sillman and He, 2002; Ran et al., 2009; Prabamroong et al., 2012; Strong et al., 2013; Zou et al., 2015; Jia et al., 2016; Li et al., 2017). In the VOC-limited (NO_x-limited) regime, O_3 decreases with decreasing VOCs (NO_x) and increases with decreasing NO_x (VOCs). In transition regime, O_3 is sensitive to both NO_x and VOCs (Milford et al., 1989; Seinfeld and Pandis, 2006). We used the typical VOCs/NO_x ratios which were applied by empirical kinetic modeling approach (EKMA) to classify sensitivity regimes during G20 to indicate the possible O_3 response to changes in VOCs or NO_x concentrations. O_3 formation can be VOC-limited if the ratios are less than 4 and can be NO_x-limited if the ratios are larger than 15. The VOCs/NO_x ratios of 4–15 indicate a transitional regime (Lou et al., 2010; Edson et al., 2017; Li et al., 2017a), with which O_3 concentrations will increase with increasing NO_x and VOCs and vice versa (Sillman, 1999).

Fig. 9 shows the simulated distribution of the ratios of VOCs/NO_x in YRD from the GEOS-Chem model averaged over 24 August to 6 September. Following Lou et al. (2010), VOCs considered include ethane, propane, alkanes with more than 4 carbon atoms, propene, ketones, Methyl ethyl ketone, isoprene, other aldehydes, aldehydes with more than 3 carbon atoms, methyl ketone, methacrolein, and formaldehyde. VOCs/NO_x ratios are simulated to be 9.9 in the core area, 17.7 in southern Zhejiang province, and 3.8 in southern Jiangsu province. Correspondingly, central and northern Anhui and southern Jiangsu were VOC-limited, western and southwestern Zhejiang were NO_x-limited, and northern, central (core area), and southeastern Zhejiang were in the transitional regime. The regimes we identified agrees with the results of previous studies using models and observations (Jin and Holloway, 2015; Li et al., 2017a; Wang et al., 2019). Therefore, reductions in either NO_x or VOCs reduced O_3 concentrations effectively in Hangzhou during G20.

It should be noted that the VOCs/NO_x ratio can only be considered as an indicator to analyze the possible ozone response to

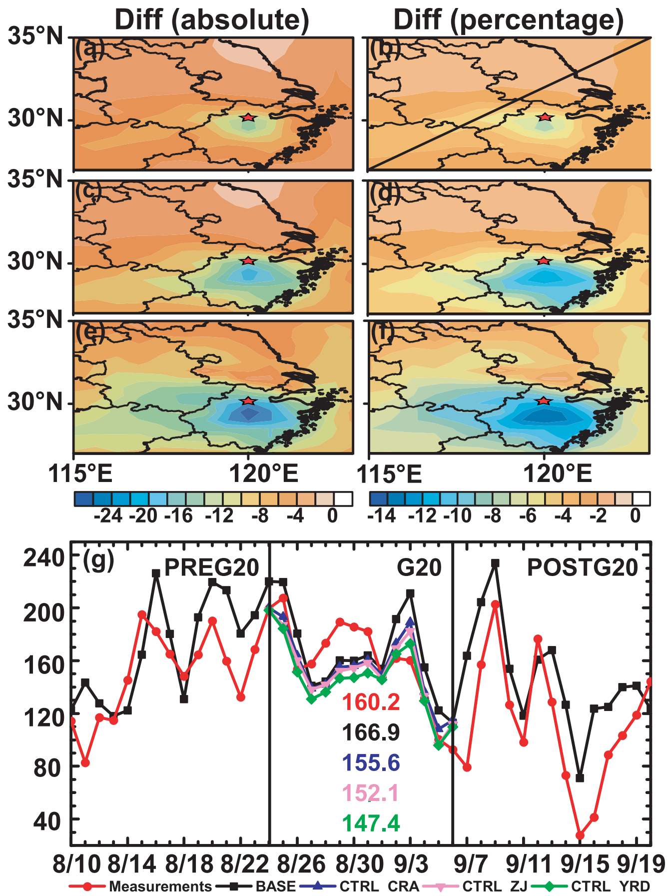

Fig. 7. (a)–(c) Absolute differences (μg m^{-3}) and (d)–(f) percentage changes (%) in MDA8 O_3 concentrations in CTRL_CRA, CTRL_ZJ, and CTRL_YRD simulations (from top to bottom) relative to the BASE simulation. (g) Comparisons of daily MDA8 O_3 concentrations (μg m^{-3}) from the BASE (black line), CTRL_CRA (blue line), CTRL_ZJ (cyan line) and CTRL_YRD (green line) simulations with observations (red line) in Hangzhou from 10 August to 20 September of 2016. The colored numbers are the averaged MDA8 O_3 concentrations (μg m^{-3}) during G20 from measurements and simulations. The red star in (a)–(f) indicates the location of Hangzhou. (For interpretation of the references to color in this figure legend, the reader is referred to the Web version of this article.)

changes in VOCs or NO_x concentrations because this rule does not account for the impact of VOCs reactivity, biogenic response, geographic variations (Sillman, 1999). The typical values for differentiating the two regimes can also be different according to regions and time periods in previous studies (Milford et al., 1994; Hanna et al., 1996; Zou et al., 2015).

3.5. *Impact of emission reductions by sectors on O_3*

According to the measurements during G20, mean concentration of MDA8 O_3 in Hangzhou (160.2 μg m^{-3}) was above the national air quality standard (Fig. 4). Extra emission reductions should be carried out to keep O_3 concentrations below national standard. It will be helpful to examine the sensitivities of O_3 concentrations in Hangzhou to emissions in different sectors (industry, power, transportation, and residential sectors) during G20. Four numerical experiments are conducted as described in Section 2.4.

Fig. 9 shows, relative to the BASE simulation, the changes in mean MDA8 O_3 concentrations in Hangzhou during G20 when emissions of a specific sector are set to zero in YRD. The emissions from industry sector play a dominant role in O_3 formation in YRD. The removal of emissions of all anthropogenic chemical species (NO_x, VOCs, CO, BC, OC, NH_3, SO_2) from industry sector would reduce MDA8 O_3 concentrations in the whole of YRD especially in Zhejiang province during G20 (Fig. 9a), with the highest reductions of 23.1 μg m^{-3} in MDA8 O_3 concentrations. Simulated distribution of reductions in MDA8 O_3 concentrations is similar to that of simulated MDA8 O_3 in the BASE simulation (Fig. S3b). The emissions of both NO_x and VOCs from industry sector are high in southern Jiangsu province, Shanghai, and northern Zhejiang province (Figs. S4a and S4e). The largest reductions in MDA8 O_3 in central Zhejiang in Fig. 9a is a result of the transitional regime in this region (Fig. 8). Concentrations of MDA8 O_3 in Hangzhou during G20 would decrease by 17.6 μg m^{-3} (10.5%) due to cutting off emissions from industry sector in YRD.

In power sector, emissions of NO_x are dominant and those of VOCs are practically zero. The highest NO_x emissions are located over Southern Jiangsu and Shanghai (Figs. S4b and S4f). The removal of emissions from power sector would have an adverse effect of increasing MDA8 O_3 concentrations by 0–6 μg m^{-3} in Southern Jiangsu and Shanghai (Fig. 9b) where VOCs/NO_x ratios exhibit a VOC-limited regime. In Hangzhou, the removal of emissions from power sector in YRD is simulated to reduce MDA8 O_3 concentrations during G20 by 5.1 μg m^{-3} (3.1%).

In transportation sector, emissions of NO_x are much higher than those of VOCs (Figs. S2e and S2g), and emissions are generally high in southern Jiangsu, Shanghai, and Hangzhou. The removal of emissions from transportation sector would reduce concentrations of MDA8 O_3 in the whole of YRD, especially in central and southern Zhejiang province where highest reductions of about 16.0 μg m^{-3} are simulated. Over southern Jiangsu and Shanghai where O_3 formation is VOC-limited, the reductions in MDA8 O_3 are small (less than 3 μg m^{-3}). Without emissions from transportation sector, concentrations of MDA8 O_3 in Hangzhou during G20 would be reduced by 12.3 μg m^{-3} (7.4%) relative to the BASE simulation.

Among the sectors considered here, residential sector has the lowest emissions of NO_x and the second lowest emissions of VOCs (Figs. S2d and S2h). Emissions of VOCs are larger than those of NO_x, so the removal of emissions from residential sector would reduce MDA8 O_3 concentrations in the whole of YRD. Reductions in MDA8 O_3 concentrations of 3–6 μg m^{-3} are simulated in northern Zhejiang, southern Jiangsu, and southern Anhui provinces. No emissions from residential sector would reduce concentrations of MDA8 O_3 in Hangzhou by 3.2 μg m^{-3} (1.9%) during G20.

In summary, to further reduce O_3 in Hangzhou, reductions in emissions from industry and transportation sectors can be the most effective. Reductions in industry sector over the strictly controlled

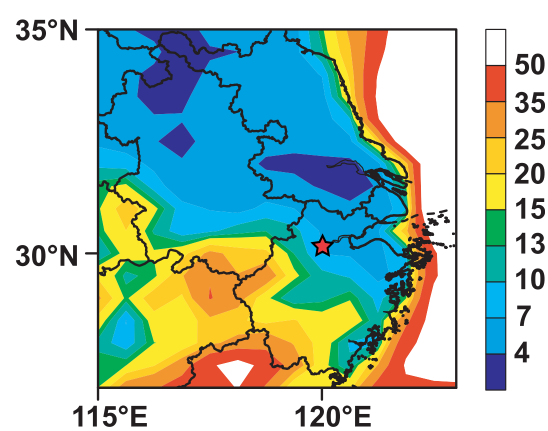

Fig. 8. Simulated distribution of the ratios of VOCs/NO_x averaged over 24 August to 6 September. The red star indicates the location of Hangzhou. (For interpretation of the references to color in this figure legend, the reader is referred to the Web version of this article.)

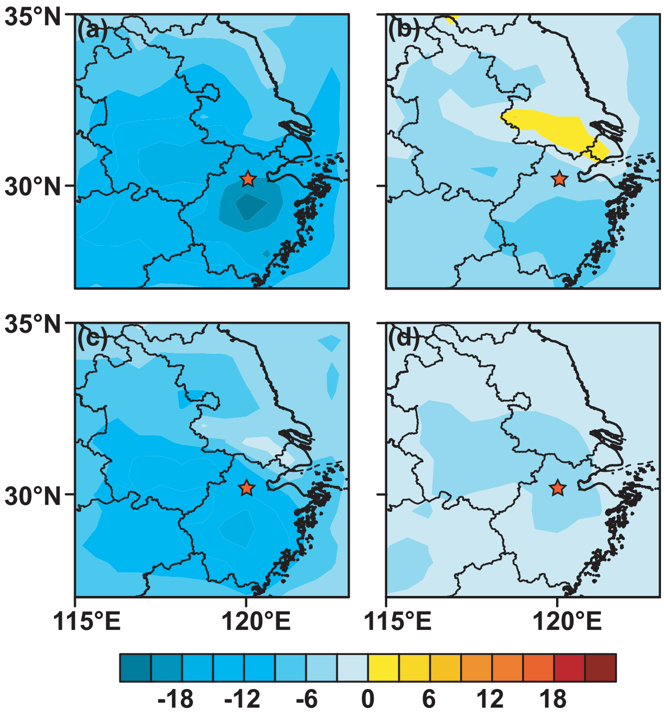

Fig. 9. Simulated mean changes in MDA8 O_3 concentrations (μg m^{-3}) during G20 in simulations (a) without emissions from industry sector (CTRL_noIND), (b) without emissions from power sector (CTRL_noPOW), (c) without emissions from transportation sector (CTRL_noTRA), and (d) without emissions from residential sector (CTRL_noRES) in YRD relative to BASE simulation. The red star in (a)–(d) indicates the location of Hangzhou. (For interpretation of the references to color in this figure legend, the reader is referred to the Web version of this article.)

area (Fig. 1) would be especially helpful for keeping the MDA8 O_3 concentrations in Hangzhou during G20 below the national standard considering the transitional regime in that region. It should be noted that the simulations with 100% emission reductions in each sector represent an ideal assumption to evaluate the impact of emission reductions by sectors on O_3. The percentage of emission reductions conducted in core area in Hangzhou of different sectors were in the range of 50%–100% during G20 (Table 1), so the actual impacts of the emission reductions conducted for the four sectors would be less than those obtained from the sensitivity studies.

4. Conclusion

Summertime O_3 concentrations have been increasing over eastern China since 2013. Here we take G20 meeting as an example to investigate whether and how the emission control measures can reduce O_3 concentrations under the typical weather condition during late summer to early fall. The emissions, concentrations, and meteorological conditions are examined from 10 August to 20 September in 2016, covering the periods of PREG20, G20, and POSTG20. The nested-grid version of the GEOS-Chem model is used to assess the effectiveness of emission control measures carried out during G20.

During G20 meeting, observed concentrations of all air pollutants were below national air quality standards except for O_3. With the emission control measures, mean MDA8 O_3 concentration was 160.2 μg m^{-3} during G20. Analyses of meteorological parameters show that the period of G20 had high temperature (27.4 °C), low relative humidity (60.4%), low wind speed (2.6 m s^{-1}) and insufficient precipitation (16.9 mm), all of which were favorable for O_3 formation.

Model evaluation shows that the GEOS-Chem model can capture well the daily variations of MDA8 O_3 in Hangzhou, with correlation coefficients (NMBs) of 0.71 (12.3%), 0.81 (−8.0%), and 0.80 (31.1%) in PREG20, G20, and POSTG20, respectively. Model simulations show that, during G20, the control measures in the core control area, Zhejiang province, and the whole of YRD lead to reductions in MDA8 O_3 in Hangzhou by 6.8%, 8.9%, and 11.7%, respectively, indicating that it is essential to carry out district-joint control measures during G20. Ratios of VOCs/NO_x in YRD during G20 indicate that the core area and most of Zhejiang province were in transitional zone ($4 \le$VOCs/$NO_x \le 15$); reductions in either NO_x or VOCs can reduce concentrations of O_3 effectively.

Sensitivities of MDA8 O_3 concentrations to emission reductions in different sectors, including industry, power, transportation, and residential sectors, are also examined. Removal of emissions of all chemical species from these sectors are simulated to reduce the MDA8 O_3 concentrations in Hangzhou during G20 by 17.6 μg m^{-3} (10.5%), 5.1 μg m^{-3} (3.1%), 12.3 μg m^{-3} (7.4%), and 3.2 μg m^{-3} (1.9%), respectively. Therefore, the control of emissions from industry and transportation sectors in YRD can be the most effective to reduce O_3 in the YRD. Considering the location and the NO_x/VOCs ratios, further reductions in industry sector in the strictly controlled area would be especially helpful to keep concentrations of O_3 in Hangzhou below the national standard during G20.

On the basis of our results, we argue that O_3 pollution can be controlled in summer by emission reductions under the background of seriously increasingly O_3 pollution in China. The effectiveness of emission control measures in Hangzhou depend on the local transitional regime of VOCs/NO_x ratios in summer, which may not be the situation in other places of eastern China. Our model results may also have uncertainties in emissions inventories and the assumed reduction rates. This work highlights the necessity of district-joint control and the sensitivities of O_3 to reductions in different sectors provide suggestions for O_3 control in YRD in the future.

Author contribution

HL and YW conceived the study and designed the experiments. YW carried out the simulations and performed the analysis. YW and HL prepared the manuscript.

Declaration of competing interest

The authors declare that they have no known competing financial interests or personal relationships that could have appeared to influence the work reported in this paper.

Acknowledgement

This work was supported by the National Key Research and Development Program of China (grant no. 2019YFA0606804) and the National Natural Science Foundation of China (grant no. 91744311).

Appendix A. Supplementary data

Supplementary data to this article can be found online at https://doi.org/10.1016/j.chemosphere.2020.127729.

References

Alexander, B., Park, R.J., Jacob, D.J., Li, Q., Yantosca, R.M., Savarino, J., Lee, C.C., Thiemens, M.H., 2005. Sulfate formation in sea-salt aerosols: constraints from

oxygen isotopes. J. Geophys. Res. 110 https://doi.org/10.1029/2004JD005659.
Atkinson, R., 1998. Atmospheric chemistry of VOCs and NO_x. Atmos. Environ. 34, 2063–2101. https://doi.org/10.1016/S1352-2310(99)00460-4.
Bey, I., Jacob, D.J., Yantosca, R.M., Logan, J.A., Field, B.D., Fiore, A.M., Li, Q., Liu, H.Y., Mickley, L.J., Schultz, M.G., 2001. Global modeling of tropospheric chemistry with assimilated meteorology: model description and evaluation. J. Geophys. Res. 106, 23073–23095. https://doi.org/10.1029/2001JD000807.
Bian, H., Prather, M.J., 2002. Fast-J2: accurate simulation of stratospheric photolysis in global chemical models. J. Atmos. Chem. 41, 281–296. https://doi.org/10.1023/A:1014980619462.
Cai, W., Li, K., Liao, H., Wang, H., Wu, L., 2017. Weather conditions conducive to Beijing severe haze more frequent under climate change. Nat. Clim. Change 7, 257–262. https://doi.org/10.1038/nclimate3249.
Edson, C.T., Iván, H.-P., Alberto, M., 2017. Use of combined observational- and model-derived photochemical indicators to assess the O_3-NO_x-VOC System sensitivity in urban areas. Atmosphere 8, 22. https://doi.org/10.3390/atmos8020022.
Evans, M.J., Jacob, D.J., 2005. Impact of new laboratory studies of N_2O_5 hydrolysis on global model budgets of tropospheric nitrogen oxides, ozone, and OH. Geophys. Res. Lett. 32 https://doi.org/10.1029/2005GL022469.
Fairlie, T.D., Jacob, D.J., Park, R.J., 2007. The impact of transpacific transport of mineral dust in the United States. Atmos. Environ. 41, 1251–1266. https://doi.org/10.1016/j.atmosenv.2006.09.048.
Fu, J.S., Streets, D.G., Jang, C., Hao, J., He, K., Wang, L., Zhang, Q., 2009. Modeling regional/urban ozone and particulate matter in beijing, China. J. Air Waste Manag. Assoc. 59, 37–44. https://doi.org/10.3155/1047-3289.59.1.37.
Gao, Y., Liu, X., Zhao, C., Zhang, M., 2011. Emission controls versus meteorological conditions in determining aerosol concentrations in Beijing during the 2008 Olympic Games. Atmos. Chem. Phys. 11, 12437–12451. https://doi.org/10.5194/acp-11-12437-2011.
Gong, C., Liao, H., 2019. A typical weather pattern for ozone pollution events in North China. Atmos. Chem. Phys. 19, 13725–13740. https://doi.org/10.5194/acp-19-13725-2019.
Gu, Y., Liao, H., 2016. Response of fine particulate matter to reductions in anthropogenic emissions in Beijing during the 2014 Asia–Pacific Economic Cooperation summit. Atmospheric Ocean. Sci. Lett. 9, 411–419. https://doi.org/10.1080/16742834.2016.1230465.
Guo, J., He, J., Liu, H., Miao, Y., Liu, H., Zhai, P., 2016. Impact of various emission control schemes on air quality using WRF-Chem during APEC China 2014. Atmos. Environ. 140, 311–319. https://doi.org/10.1016/j.atmosenv.2016.05.046.
Hanna, S.R., Moore, G.E., Fernau, M.E., 1996. Evaluation of photochemical grid models (UAM-IV, UAM-V, and the ROM/UAM-IV couple) using data from the lake Michigan ozone study (LMOS). Atmos. Environ. 30, 3265–3279. https://doi.org/10.1016/1352-2310(96)00060-X.
Huang, Q., Tijian, W., Pulong, C., Xiaoxian, H., Jialei, Z., Bingliang, Z., 2017. Impacts of emission reduction and meteorological conditions on air quality improvement during the 2014 Youth Olympic Games in Nanjing, China. Atmos. Chem. Phys. 1–19 https://doi.org/10.5194/acp-17-13457-2017.
Huang, R., Zhang, Y., Bozzetti, C., Ho, K., Cao, J., Han, Y., Daellenbach, K.R., Slowik, J.G., Platt, S.M., Canonaco, F., 2014. High secondary aerosol contribution to particulate pollution during haze events in China. Nature 514, 218–222. https://doi.org/10.1038/nature13774.
Jacob, D.J., 2000. Heterogeneous chemistry and tropospheric ozone. Atmos. Environ. 34, 2131–2159. https://doi.org/10.1016/S1352-2310(99)00462-8.
Jia, C., Mao, X., Huang, T., Liang, X., Wang, Y., Shen, Y., Jiang, W., Wang, H., Bai, Z., Ma, M., 2016. Non-methane hydrocarbons (NMHCs) and their contribution to ozone formation potential in a petrochemical industrialized city, Northwest China. Atmos. Res. 169, 225–236. https://doi.org/10.1016/j.atmosres.2015.10.006.
Jin, X., Holloway, T., 2015. Spatial and temporal variability of ozone sensitivity over China observed from the Ozone Monitoring Instrument. J. Geophys. Res. 120, 7229–7246. https://doi.org/10.1002/2015JD023250.
Li, K., Chen, L., Ying, F., White, S.J., Jang, C., Wu, X., Gao, X., Hong, S., Shen, J., Azzi, M., 2017a. Meteorological and chemical impacts on ozone formation: a case study in Hangzhou, China. Atmos. Res. 196, 40–52. https://doi.org/10.1016/j.atmosres.2017.06.003.
Li, K., Liao, H., Zhu, J., Moch, J.M., 2016a. Implications of RCP emissions on future $PM_{2.5}$ air quality and direct radiative forcing over China. J. Geophys. Res. 121 https://doi.org/10.1002/2016JD025623.
Li, L., An, J., Shi, Y.Y., Zhou, M., Yan, R., Huang, C., Wang, H., Lou, S., Wang, Q., Lu, Q., 2016b. Source apportionment of surface ozone in the Yangtze River Delta, China in the summer of 2013. Atmos. Environ. 144, 194–207. https://doi.org/10.1016/j.atmosenv.2016.08.076.
Li, P., Wang, L., Guo, P., Yu, S., Mehmood, K., Wang, S., Liu, W., Seinfeld, J.H., Zhang, Y., Wong, D.C., 2017b. High reduction of ozone and particulate matter during the 2016 G-20 summit in Hangzhou by forced emission controls of industry and traffic. Environ. Chem. Lett. 15, 709–715. https://doi.org/10.1007/s10311-017-0642-2.
Li, X., Qiao, Y., Zhu, J., Shi, L., Wang, Y., 2017c. The "APEC blue" endeavor: causal effects of air pollution regulation on air quality in China. J. Clean. Prod. 168, 1381–1388. https://doi.org/10.1016/j.jclepro.2017.08.164.
Liang, P., Zhu, T., Fang, Y., Li, Y.P., Han, Y., Wu, Y., Hu, M., Wang, J., 2017. The role of meteorological conditions and pollution control strategies in reducing air pollution in Beijing during APEC 2014 and Victory Parade 2015. Atmos. Chem. Phys. 17, 13921–13940. https://doi.org/10.5194/acp-17-13921-2017.
Liu, H., Jacob, D.J., Bey, I., Yantosca, R.M., 2001. Constraints from ^{210}Pb and ^{7}Be on wet deposition and transport in a global three-dimensional chemical tracer model driven by assimilated meteorological fields. J. Geophys. Res. 106, 12109–12128. https://doi.org/10.1029/2000JD900839.
Lou, S., Zhu, B., Liao, H., 2010. Impacts of O_3 precursor on surface O_3 concentration over China. Trans. Atmos. Sci. 451–459, 033.
Mao, M., Hu, D., 2017. Evaluation of the air pollution control over Zhejiang province during the G20 summit in Hangzhou. Res. Environ. Sci. 30.
Milford, J.B., Russell, A.G., Mcrae, G.J., 1989. A new approach to photochemical pollution control: implications of spatial patterns in pollutant responses to reductions in nitrogen oxides and reactive organic gas emissions. Environ. Sci. Technol. 23, 1290–1301. https://doi.org/10.1021/es00068a017.
Milford, J.B., Gao, D., Sillman, S., Blossey, P.N., Russell, A.G., 1994. Total reactive nitrogen (NOy) as an indicator of the sensitivity of ozone to reductions in hydrocarbon and NOx emissions. J. Geophys. Res. 99, 3533–3542. https://doi.org/10.1029/93JD03224.
Ni, R., Lin, J., Yan, Y., Lin, W., 2018a. Foreign and domestic contributions to springtime ozone over China. Atmos. Chem. Phys. 18, 1–39. https://doi.org/10.5194/acp-2017-1226.
Ni, Z., Luo, K., Gao, Y., Jiang, F., Gao, X., Fan, J., Chen, C., 2018b. Modeling tropospheric O_3 evolution during the 2016 Group of twenty summit in Hangzhou, China. Atmos. Chem. Phys. 1–25. https://doi.org/10.5194/acp-2018-76.
Park, R.J., Jacob, D.J., Chin, M., Martin, R.V., 2003. Sources of carbonaceous aerosols over the United States and implications for natural visibility. J. Geophys. Res. 108 https://doi.org/10.1029/2002JD003190.
Park, R.J., Jacob, D.J., Field, B.D., Yantosca, R.M., Chin, M., 2004. Natural and transboundary pollution influences on sulfate-nitrate-ammonium aerosols in the United States: implications for policy. J. Geophys. Res. 109 https://doi.org/10.1029/2003JD004473.
Prabamroong, T., Manomaiphiboon, K., Limpaseni, W., Sukhapan, J., Bonnet, S., 2012. Ozone and its potential control strategy for Chon Buri city, Thailand. J. Air Waste Manag. Assoc. 62, 1411–1422. https://doi.org/10.1080/10962247.2012.716385.
Pye, H.O.T., Liao, H., Wu, S., Mickley, L.J., Jacob, D.J., Henze, D.K., Seinfeld, J.H., 2009. Effect of changes in climate and emissions on future sulfate-nitrate-ammonium aerosol levels in the United States. J. Geophys. Res. 114 https://doi.org/10.1029/2008JD010701.
Qiu, Y., Liao, H., Zhang, R., Hu, J., 2017. Simulated impacts of direct radiative effects of scattering and absorbing aerosols on surface layer aerosol concentrations in China during a heavily polluted event in February 2014. J. Geophys. Res. 122, 5955–5975. https://doi.org/10.1002/2016JD026309.
Rabl, A., Eyre, N., 1998. An estimate of regional and global O_3 damage from precursor NO_x and VOC emissions. Environ. Int. 24, 835–850. https://doi.org/10.1016/S0160-4120(98)00053-1.
Ran, L., Zhao, C., Geng, F., Tie, X., Tang, X., Peng, L., Zhou, G., Yu, Q., Xu, J., Guenther, A., 2009. Ozone photochemical production in urban Shanghai, China: analysis based on ground level observations. J. Geophys. Res. 114 https://doi.org/10.1029/2008JD010752.
Seinfeld, J.H., Pandis, S.N., 2006. Atmospheric Chemistry and Physics: from Air Pollution to Climate Change, second ed. John Wiley & Sons, New York.
Shao, M., Zhang, Y., Zeng, L., Tang, X., Zhang, J., Zhong, L., Wang, B., 2009. Ground-level ozone in the pearl River Delta and the roles of VOC and NO_x in its production. J. Environ. Manag. 90, 512–518. https://doi.org/10.1016/j.jenvman.2007.12.008.
Sillman, S., 1999. The relation between ozone, NO_x and hydrocarbons in urban and polluted rural environments. Atmos. Environ. 33, 1821–1845. https://doi.org/10.1016/S1352-2310(98)00345-8.
Sillman, S., He, D., 2002. Some theoretical results concerning O_3-NO_x-VOC chemistry and NO_x-VOC indicators. J. Geophys. Res. 107 https://doi.org/10.1029/2001JD001123.
Strong, J., Whyatt, J.D., Metcalfe, S.E., Derwent, R.G., Hewitt, C.N., 2013. Investigating the impacts of anthropogenic and biogenic VOC emissions and elevated temperatures during the 2003 ozone episode in the UK. Atmos. Environ. 74, 393–401. https://doi.org/10.1016/j.atmosenv.2013.04.006.
Su, W., Liu, C., Hu, Q., Fan, G., Xie, Z., Huang, X., Zhang, T., Chen, Z., Dong, Y., Ji, X., 2017. Characterization of ozone in the lower troposphere during the 2016 G20 conference in Hangzhou. Sci. Rep. 7 https://doi.org/10.1038/s41598-017-17646-x, 17368-17368.
Tang, G., Zhu, X., Xin, J., Hu, B., Song, T., Sun, Y., Zhang, J., Wang, L., Cheng, M., Chao, N., 2017. Modelling study of boundary-layer ozone over northern China - Part I: ozone budget in summer. Atmos. Res. 187, 128–137. https://doi.org/10.1016/j.atmosres.2016.10.017.
Thornton, J.A., Jaegle, L., Mcneill, V.F., 2008. Assessing known pathways for HO_2 loss in aqueous atmospheric aerosols: regional and global impacts on tropospheric oxidants. J. Geophys. Res. 113 https://doi.org/10.1029/2007JD009236.
Wang, P., Chen, Y., Hu, J., Zhang, H., Ying, Q., 2019. Attribution of tropospheric ozone to NO_x and VOC emissions: considering ozone formation in the transition regime. Environ. Sci. Technol. 53, 1404–1412. https://doi.org/10.1021/acs.est.8b05981.
Wang, S., Zhao, M., Xing, J., Ye, W.U., Zhou, Y.U., Lei, Y.U., Kebin, H.E., Lixin, F.U., Hao, J., 2010. Quantifying the air pollutants emission reduction during the 2008 olympic games in beijing, 44. Environmental Science & Technology, pp. 2490–2496. https://doi.org/10.1021/es9028167.
Wang, Y., Hao, J., Mcelroy, M.B., Munger, J.W., Ma, H., Chen, D., Nielsen, C.P., 2009. Ozone air quality during the 2008 Beijing Olympics: effectiveness of emission restrictions. Atmos. Chem. Phys. 9, 5237–5251. https://doi.org/10.5194/acp-9-

5237-2009.
Wei, W., Cheng, S., Li, G., Wang, G., Wang, H., 2014. Characteristics of ozone and ozone precursors (VOCs and NO_x) around a petroleum refinery in Beijing, China. J. Environ. Sci. China 26, 332–342. https://doi.org/10.1016/S1001-0742(13)60412-X.
Wesely, M.L., 1989. Parameterization of surface resistances to gaseous dry deposition in regional-scale numerical models. Atmos. Environ. 23, 1293–1304. https://doi.org/10.1016/j.atmosenv.2007.10.058.
Xu, R., Tang, G., Wang, Y., Tie, X., 2016. Analysis of a long-term measurement of air pollutants (2007-2011) in north China plain (NCP); impact of emission reduction during the beijing olympic games. Chemosphere 159, 647–658. https://doi.org/10.1016/j.chemosphere.2016.06.025.
Yang, Y., Liao, H., Li, J., 2014. Impacts of the East Asian summer monsoon on interannual variations of summertime surface-layer ozone concentrations over China. Atmos. Chem. Phys. 14, 6867–6879. https://doi.org/10.5194/acp-14-6867-2014.
Yang, Y., Liao, H., Lou, S., 2016. Increase in winter haze over eastern China in recent decades: roles of variations in meteorological parameters and anthropogenic emissions. J. Geophys. Res. 121 https://doi.org/10.1002/2016JD025136.
Yu, H., Dai, W., Ren, L., Liu, D., Yan, X., Xiao, H., He, J., Xu, H., 2018. The effect of emission control on the submicron particulate matter size distribution in Hangzhou during the 2016 G20 summit. Aerosol Air Qual. Res. 18, 2038–2046. https://doi.org/10.4209/aaqr.2018.01.0014.
Zhang, G., Xu, H., Wang, H., Xue, L., He, J., Xu, W., Qi, B., Du, R., Liu, C., Li, Z., 2020. Exploring the inconsistent variations in atmospheric primary and secondary pollutants during the G20 2016 Summit in Hangzhou, China: implications from observation and model. Atmos. Chem. Phys. 1–25. https://doi.org/10.5194/acp-2019-1061.
Zhang, L., Liu, L., Zhao, Y., Gong, S., Zhang, X., Henze, D.K., Capps, S.L., Fu, T., Zhang, Q., Wang, Y., 2015. Source attribution of particulate matter pollution over North China with the adjoint method. Environ. Res. Lett. 10, 084011 https://doi.org/10.1088/1748-9326/10/8/084011.
Zhang, L., Shao, J., Lu, X., Zhao, Y., Hu, Y., Henze, D.K., Liao, H., Gong, S., Zhang, Q., 2016. Sources and processes affecting fine particulate matter pollution over North China: an adjoint analysis of the Beijing APEC period. Environ. Sci. Technol. 50, 8731–8740. https://doi.org/10.1021/acs.est.6b03010.
Zhu, J., Chen, L., Liao, H., Dang, R., 2019. Correlations between $PM_{2.5}$ and ozone over China and associated underlying reasons. Atmosphere 10, 352. https://doi.org/10.3390/atmos10070352.
Zhu, J., Liao, H., 2016. Future ozone air quality and radiative forcing over China owing to future changes in emissions under the Representative Concentration Pathways (RCPs). J. Geophys. Res. 121, 1978–2001. https://doi.org/10.1002/2015JD023926.
Zou, Y., Deng, X.J., Zhu, D., Gong, D.C., Wang, H., Li, F., Tan, H.B., Deng, T., Mai, B.R., Liu, X.T., Wang, B.G., 2015. Characteristics of 1 year of observational data of VOCs, NO_x and O_3 at a suburban site in Guangzhou, China. Atmos. Chem. Phys. 15, 6625–6636. https://doi.org/10.5194/acp-15-6625-2015.